Songklanakarin J. Sci. Technol.
44 (2), 488-495, Mar. - Apr. 2022

http://www.sjst.psu.ac.th

Original Article

Formulation and physicochemical properties of resveratrol-loaded lipid-nanocarriers

Benchawan Chamsai[1], Praneet Opanasopit[2], Pornsak Sriamornsak[2], Chitralada Vasarach[1], and Wipada Samprasit[1*]

[1] *Department of Pharmaceutical Technology, College of Pharmacy, Rangsit University, Mueang, Pathum Thani, 12000 Thailand*

[2] *Department of Pharmaceutical Technology, Faculty of Pharmacy, Silpakorn University, Mueang, Nakhon Pathom, 73000 Thailand*

Received: 2 August 2021; Revised: 1 October 2021; Accepted: 7 October 2021

Abstract

The study aimed to prepare and evaluate the physicochemical properties of resveratrol (Res)-loaded lipid-nanocarriers including nanostructured lipid carriers (NLCs) and nanoemulsions (NEs). The effects of composition and process parameters on the physicochemical properties were demonstrated. The optimal formulation was selected to prepare the nanocarrier gels. The possible use of the lipid-nanocarriers in gels and their physical appearances was observed by visual inspection. The results showed that small carriers were prepared by homogenization at 6000 rpm for 5 min. The emulsifier system of Tween®80, Span®80 and diethylene glycol monoethyl ether (DGME) provided good physical stability. The NEs could be prepared for Res-loaded NE gels (NEGs) with minimum particle size and optimal zeta potential. Alkyl acrylate crosspolymer (PPM) was the best gelling agent in the formulation. Moreover, the blend of NE and gels (NEGs) was easy to spread on the skin with good occlusive property. Thus, these NEGs have a potential to a nanocarrier for topical delivery of Res.

Keywords: resveratrol, lipid-nanocarriers, gels, nanostructured lipid carriers, nanoemulsions

1. Introduction

Nowadays, many researchers are focusing on improving percutaneous absorption of drugs by utilizing advantages of lipid-based nanocarriers such as nanostructured lipid carriers (NLCs) and nanoemulsions (NEs). NLCs are composed of a mixture of liquid and solid lipids which can encapsulate drugs with high efficiency. Moreover, the combination of lipids and the small particle size could effectively enhance the drug absorption and lead to a passive targeting of the tissues (Wei *et al.*, 2018). NEs consist of two immiscible liquids, stabilized by an interfacial film consisting of a surfactant and co-surfactant to form a single phase. The small droplet size of NEs allows uniform deposition and penetration of drugs through the skin surface. However, some undesirable appearances are unacceptable to consumers such as the stickiness of lipid. Therefore, the use of nonsticky occlusive agents is rising. In order to formulate a topical dosage form having desired properties, NEs and NLCs can be incorporated into gels to form nanocarrier gels. The nanocarrier gel creates a monolayered lipid film onto the skin, which prevents trans-epidermal water loss, and thus it causes an occlusive effect and enhances the skin moisture content and keeps the skin hydrated (Imran. *et al.*, 2020).

Resveratrol (Res) (3,5,4′-trihydroxystilbene), a natural polyphenolic flavonoid shows beneficial effects on human health, i.e. antioxidant activity on the skin (Loureiro *et al.*, 2017). However, the application of Res is limited by its poor water solubility and its sensitivity to several environmental factors like pH and UV irradiation (Juškaité *et al.*, 2017). Lipid-nanocarriers have drawn much attention for enhancing the skin permeation of drugs owing to their

*Corresponding author
Email address: wipada.s@rsu.ac.th; swipada@hotmail.com

submicron size and their interaction with the stratum corneum (Rigon *et al.*, 2016). The lipid-nanocarriers may increase Res solubility, skin penetration and stability. Moreover, these delivery systems have the ability to protect Res during its transit inside the organism, which is extremely important to preserve its pharmacological properties (Neves *et al.*, 2013). Therefore, the novelty of this work was to systematically find the proper lipid-based nanocarriers including NEs and NLCs for Res delivery with desirable physicochemical properties. Gel-based nanocarriers were applied to improve the physical properties of dosage forms. The effects of composition and process parameters on the physicochemical properties of lipid-nanocarriers were demonstrated. The optimal formulation was selected to prepare the nanocarrier gels. The possible use of lipid-nanocarriers in the various gel types and their physical appearances was observed by visual inspection. The lipid-nanocarriers and nanocarrier gels were evaluated for particle size, zeta potential, pH, conductivity, spreadability, *in vitro* occlusive property, and stability.

2. Materials and Methods

2.1 Materials

Res (99 %) was obtained from Sami Lab Ltd., Tumkur, China. Palmitic acid (PA) and myristic acid (MA) were purchased from Aladdin Chemistry Co. Ltd. (Shanghai, China). Polysorbate (Tween®40, 60 and 80), Sorbitan esters (Span®40, 60 and 80), polyethylene glycol (PEG) 400, carbomer (carbopol®940, C) and hydroxypropyl methylcellulose 4000 (HPMC 4000, H) were bought from P.C. Drug Center (Bangkok, Thailand). Caprylic/capric glyceride (Imwitor®812, CCG) was purchased from Sasol (Hamburg, Germany). Sodium stearoyl glutamate (Emulgin®SG, ESG), alkyl acrylate crosspolymer (Propolymer™, PPM) and Aloe Vera extract (aloe barbadensis extract) were purchased from Chanjao Longevity Co., Ltd. (Bangkok, Thailand). Diethylene glycol monoethyl ether (Transcutol®, DGME) was purchased from Sigma-Aldrich (USA). Deionized (DI) water was used throughout the study and all other reagents used were of analytical grade.

2.2 Optimization of preparation process and formulation of Res-loaded lipid-nanocarriers

Res-loaded lipid-nanocarriers including NLCs and NEs were prepared by high shear homogenization and ultrasonication processes according to the previous study (Chamsai, Samprasit, Opanasopit, Benjasirimongkol, & Sriamornsak, 2020). The lipids selection was based on the Res solubility in liquid and molten solid lipids. The previous study revealed that CCG provided a high solubility of Res (Benjasirimongkol & Sriamornsak, 2016). Furthermore, the use of PA and MA made small sized NLCs (Chamsai *et al.*, 2020). The surfactants were selected on the basis of emulsification capacity to emulsify the optimized binary mixture of lipids. Briefly, a certain amount of lipid phase and surfactants were blended and heated up to form a homogenous and clear oil at 70 ± 2 °C. Res was dissolved in the hot melted lipid phase. The lipid phase was then mixed in a hot aqueous surfactant solution of temperature (75 ± 2 °C) by a homogenizer (IKA®, T 25 digital Ultra-Turrax® homogenizer, Staufen, Germany), at various speeds (4000, 6000 and 10000 rpm) for various times (5, 15 and 25 min). The obtained formulation was further treated by probe-type sonicator (A Vibra-CellTM Ultrasonic Liquid Processor VCX 130; Sonics & Materials Inc., Newtown, CT, USA). The compositions of the obtained lipid-nanocarriers are shown in Table 1. The temperature of preparation process agreed with the previous study that prepared the NLCs containing phenolic compounds by heating up to 70 ºC (Imran. *et al.*, 2020). These results supported that Res was stable under the conditions during preparation.

The lipid-nanocarriers were dispersed in the aqueous solution. The nine different areas of lipid-nanocarriers were arbitrarily recorded by an optical microscope (Motic, BA300, Texas, United States). The approximately fifty droplets per lipid-nanocarrier were also measured for the hydrodynamic diameter (HD) using image analysis software (JMicro Vision V.1.2.7, Switzerland). The mean diameter of lipid-nanocarriers was obtained by calculating the average of fifty diameters.

Table 1. Compositions of Res-loaded lipid-nanocarriers

Component (%w/w)	NLCs										NEs	
	A*	B	C	D	E	F	G	H	I	J	K	L
Res	0.2	0.2	0.2	0.2	0.2	0.2	0.2	0.2	0.4	0	0.4	0
CCG	12	12	12	12	12	12	12	12	12	12	16	16
PA	28	28	28	28	28	28	28	28	28	28	7	7
MA	-	-	-	-	-	-	-	-	-	-	7	7
Tween®40	-	-	5	-	-	-	-	-	-	-	-	-
Span®40	-	-	5	-	-	-	-	-	-	-	-	-
Tween®60	-	5	-	-	-	-	-	-	-	-	-	-
Span®60	-	5	-	-	-	-	-	-	-	-	-	-
Tween®80	5	-	-	7	3	5	5	5	5	5	4	4
Span®80	5	-	-	3	7	5	5	5	5	5	4	4
DGME	-	-	-	-	-	2.5	5	7.5	7.5	7.5	7.5	7.5
ESG	-	-	-	-	-	-	-	-	-	-	4	4
DI water qs to	100	100	100	100	100	100	100	100	100	100	100	100

* varying speed (4000, 6000 and 10000 rpm) and time (5, 15 and 25 min) of the homogenized process

2.3 Preparation of Res-loaded nanocarrier gels

The optimal Res-loaded NLCs and NEs were selected for nanocarrier gels according to a previous study with slight modification (Kaur *et al.*, 2017). Res-loaded nanocarrier gels were prepared as described in section 2.2. The lipid phase was heated up and then mixed in a hot aqueous surfactant solution containing a gel base. The C, H and PPM were dispersed into the hot aqueous surfactant solution with the Aloe Vera extract. The mixture was blended using a homogenizer at 6000 rpm for 5 min and further treated by probe-type sonicator. The Res-loaded gels were also prepared as the control by dissolving Res in PEG 400 and incorporating them into gel bases. The compositions of the nanocarrier gels are shown in Table 2.

Table 2. Compositions of Res-loaded nanocarrier gels

Component (%w/w)	NLC gels (NLCGs)		NE gels (NEGs)		Gels
	Res	Blank	Res	Blank	
Res	0.4	0	0.4	0	0.4
CCG	12	12	16	16	-
PA	28	28	7	7	-
MA	-	-	7	7	-
Tween®80	5	5	4	4	-
Span®80	5	5	4	4	-
DGME	7.5	7.5	7.5	7.5	-
ESG	-	-	4	4	-
PEG400	-	-	-	-	6
Gelling agent (C,H or PPM)	0.5	0.5	0.5	0.5	0.5
Aloe Vera extract	40	40	40	40	40
DI water qs to	100	100	100	100	100

2.4 Physicochemical characterization

2.4.1 Fourier transform infrared (FTIR) spectroscopy

The interactions between Res and all ingredients of lipid-nanocarriers were characterized using a FTIR (Nicolet 4700, USA) in the wavenumber range of 400–4000 cm^{-1}. A small number of samples was blended with potassium bromide (KBr), ground well using mortar and pestle. KBr disk was compacted using a hydraulic press. The disk was placed in the FTIR sample holder and the spectra of the samples were collected.

2.4.2 Particle size, polydispersity index (PDI) and zeta potential

The particle size, PDI, and zeta potential of Res-loaded lipid-nanocarriers were determined by Dynamic Light Scattering (ZetasizerNano-ZS90, Malvern Instruments, Malvern, UK).

2.4.3 pH and conductivity determination

The pH of all formulations was measured at 25°C using a calibrated Mettler Toledo Electrode (Mettler Toledo GmbH, Switzerland) to ensure nonirritating formulations for the skin. The conductivity of Res-loaded lipid-nanocarriers was also determined by a conductivity meter (PT-20C, Sartorius®, Germany) for indicating the characteristics of the continuous phase of the formulation.

2.4.4 Spreadability

The spreadability of Res-loaded lipid-nanocarriers was evaluated with a modified method from Arora, Aggarwal, Harikumar, and Kaur (2014). The sample was placed at the center of a glass plate, then another glass plate was placed on top for compressing. After two minutes, the spread area diameter of the sample was measured. The increase in diameter as a result of weights added leading to the spreading of sample was noted. The spreadability can be calculated as follows:

$$\text{Spreadability} = (M \times L) / T \quad (1)$$

where M was weight placed on a glass plate, L was the length of increase in diameter, and T was the time. Spreadability was presented in g cm/min.

2.4.5 *In vitro* occlusive property

The modified *in vitro* occlusion test was performed according to the previous study (López-García & Ganem-Rondero, 2015). Briefly, purified water was filled into a beaker. A cellulose filter paper (Whatman® filter paper number 1, Sigma-Aldrich, USA) was carefully covered on the beaker and was sealed by tape. Each formulation was spread on the filter surface to obtain a thin film. Beakers with the formulation were stored at 32˚C to mimic the temperature of the skin surface. The weight of the remaining water was weighted at 6 h to calculate water evaporation through the filter paper in terms of water loss. The beaker covered with the filter paper was used as a reference. The occlusion factor was calculated as follows:

$$\text{Occlusion factor} = ((R - S) / R) \times 100\ \% \quad (2)$$

where R was the water weight loss of reference and S was the water weight loss of sample.

2.4.6 Stability study

Res-loaded lipid-nanocarriers were stored to protect from light at 4 ± 2˚C according to ICH guideline. The visual appearance, particle size and zeta potential were measured at 3 months.

2.5 Statistical analysis

The results were analyzed using one-way analysis of variance (ANOVA) followed by Tukey's test. A p-value < 0.05 was considered statistically significant.

3. Results and Discussion

3.1 Factors affecting HD of Res-loaded lipid-nanocarriers

Particle size, surface charge density and shape are the important parameters for the stability of colloidal systems and the interactions of the particles with cells and tissues (Vinothini, & Rajan, 2019). The HD of NLCs was preliminarily evaluated to estimate the particle size. Figure 1 shows the HD distribution of the NLC dispersion. The first is to examine the influence of homogenization condition on the HD of NLCs. The effect of homogenizing speed was investigated in the range from 6,000 to 10,000 rpm at a constant time of 5 min. As shown in Figure 1(a), the HD of NLC did not vary significantly when the homogenizing speed was raised. The homogenizing speed imparted mechanical energy to break down the oil droplets and produce small droplets. However, high homogenizing speed may increase the likelihood of droplet coalescence by increasing droplet velocity and collision rate (Aravand & Semsarzadeh, 2008). The homogenizing time was varied from 5 to 25 min, while homogenizing speed (6000 rpm) was kept constant. The HD of NLCs was significantly affected by homogenizing time (Figure 1(b)). Increasing the time provided more energy to break down the droplets of NLCs, resulting in smaller HD of NLCs. However, the prolonged time may increase temperature, decrease the viscosity of the continuous aqueous phase and allow coalescence of the small droplets (Bamba *et al.*, 2018). For 15 and 25 min homogenizing times, the color of NLCs changed from white to grayish, which might be due to leakage of Res from the lipid component (Kubo, Augusto, & Cristianini, 2013). As a result, an appropriate homogenizing speed and time must be achieved so that the droplet size remains small, therefore, the homogenizing speed of 6,000 rpm for 5 min imparted enough mechanical energy to produce small NLCs.

The influence of the surfactant system on the HD is displayed in Figure 1(c). Tween® was used together with and Span® at the same serial number, 80, 60 or 40, in the formulations A, B and C, respectively. Due to the different hydrocarbon chains of surfactants, the HD of NLCs changed significantly. The structures of Tween®40/Span®40 have shorter chain length hydrocarbon tails than Tween®60/ Span®60 and Tween®80/Span®80, so the NLC of formulation C had the smallest HD (Khoee & Yaghoobian, 2009). However, the instability of formulations B and C was observed with creaming phenomena. Thus, the concentration of Tween®80/Span®80 was varied to minimize the HD of NLC (formulations A, D and E). HD of NLC decreased when the concentration of Span®80 was increased at a constant Tween®80/Span®80 ratio, ranking the formulations as E < A < D (Figure 1(c)). The hydrophilic-lipophilic balance between type and concentration of surfactant may be the main effect on the HD. The increase of Span®80 concentration resulted in an increase of hydrophobic groups and small droplets of NLC (Khoee & Yaghoobian, 2009). Moreover, the higher concentration of Tween®80 promoted a large interfacial area according to the ethylene oxide chain and an increase in the HD. Nevertheless, the same concentration of Tween®80 and Span®80 was the most physically stable and was selected to develop the further NLCs. DGME was used as the co-surfactant in NLCs formulation. When the DGME was added, the HD became smaller (F, G, H < A). A higher surfactant concentration covered the surface of the lipid phase, decreased the interfacial tension and resulted in a smaller HD (Subramaniam, Siddik, & Nagoor, 2020). When the concentration of DGME was increased, the HD became insignificantly smaller. The formulation H with the DGME at 7.5 % showed the smallest HD (Figure 1(c)). Moreover, increasing the Res from 0.2 % to 0.4 % provided an insignificant difference in the HD. These outcomes can be attributed to the Res being dissolved within the lipid matrix and acting as a co-surfactant, which had a negative correlation

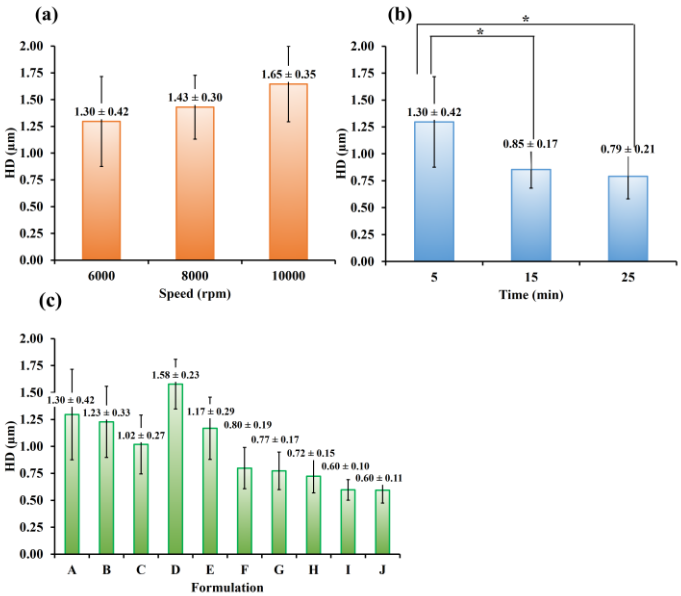

Figure 1. HD of NLCs as affected by the factors: (a) homogenizing speed, (b) homogenizing time, and (c) formulation. *statistically significant ($p < 0.05$)

with HD (Souza *et al.*, 2011). Formulations J and I represented the blank and Res-loaded NLCs at 0.4 %, respectively. Then, Res-loaded NEs were also prepared by the same techniques. The optimized homogenizing condition and surfactant system was used. ESG was also used as an auxiliary surfactant in the formulations. Formulations L and K were represented the blank and Res-loaded NEs, respectively.

3.2 Physicochemical characterizations of Res-loaded nanocarrier gels

The lipid-nanocarriers I, J, K and L were selected to prepare Res-loaded nanocarrier gels. The use of C and H in the formulation provided less stability with the appearance of creaming, as seen in Figure 2(a) and (b). On the other hand, PPM favored the physical characteristics and good stability (Figure 2(c)). PPM is an anionic polymer which has co-surfactant-like properties, resulting in a homogeneous and stable formulation. Thus, PPM was used as a gel base for NLCs and NEs formulations, namely in NLC gels (NLCGs) and NE gels (NEGs). When the lipid phase of NLCs was homogenized with hot aqueous surfactant solution containing PPM, the mixture was highly viscous and difficult to mix. However, this was not the case with NEGs preparation. The solid lipid of NEs formulation had two times lower content than in NLCs (Table 2). Thus, nanocarrier gels could be prepared as Res-loaded NEGs to compare physicochemical properties with Res-loaded NLCs and Res-loaded gels.

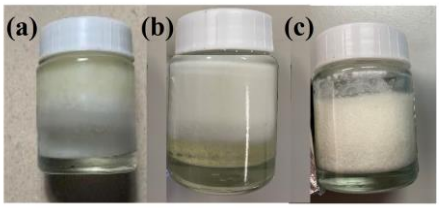

Figure 2. Physical appearances of Res-loaded NEGs with alternative gelling agents: (a) C, (b) H, and (c) PPM after storage at room temperature for 7 days

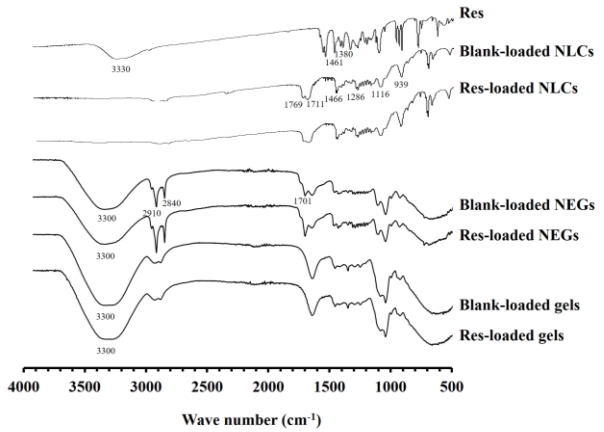

Figure 3. FTIR spectra of Res powder, blank, and Res-loaded nanocarriers and gels

3.2.1 FTIR

The FTIR spectra of Res powder, blank and Res-loaded lipid-nanocarriers are shown in Figure 3. Res showed absorption peaks at 1461 cm^{-1} (aromatic hydrocarbon), 1380 cm^{-1} (CC stretching vibrations) and broad band of O-H stretching at 3300 cm^{-1} that demonstrated the trans-form of Res, which matches prior literature (Venuti *et al.*, 2014). The characteristic peaks of blank-loaded NLCs were the peaks of PA at 2676, 1769, 1711 1466, 1462, 1413, 1379, 1286, 1240, 1116, 1108 and 939 cm^{-1} (Han & Wang, 2016). Whereas, the characteristic peaks of blank-loaded NEGs were the peaks of PA and MA acid, which corresponded to C=O stretching vibrations at 1701 cm^{-1} (Trivedi *et al.*, 2015). The peaks at 2910 and 2840 cm^{-1} of NEGs presented the characteristic of PPM (Jiang *et al.*, 2013). Moreover, a board band around 3200 cm^{-1} indicated O-H stretching of the aqueous phase of NEGs. In the case of blank-loaded gels, a broad spectrum of O-H stretching and the characteristic peak of PPM were found. For the Res-loaded NLCs, NEGs and gels, the peaks related to functional groups of Res were masked by the stronger signal of carriers without predominant shifting of peaks or creation of new peaks, indicating Res entrapment in the lipid matrix of NLCs, and NEGs or dissolving in the gel bases.

3.2.2 Particle size, PDI and zeta potential

Particle size is the major characteristic for the evaluation of lipid-nanocarriers (Vinothini, & Rajan, 2019). Table 3 shows that NLCs and NEGs had particle sizes ranging from 160.0 to 346.7 nm. This size range was appropriate for topical Res delivery. The lipid-nanocarriers might be localized and could enter in the skin to increase of skin permeation of Res. Nanoparticles with sizes smaller than 500 nm are generally internalized by receptor mediated endocytosis (Vinothini, & Rajan, 2019). Significantly larger particle size of NLCs than of NEGs was found. This might be because the different lipid types and ratios in lipid core of these carriers. Moreover, a decrease in particle size occurred when Res was loaded into the lipid-nanocarriers. Res, acted as co-surfactant and hence had a negative correlation with particle size (Souza *et al.*, 2011). Res might reduce the interfacial tension and help in the stabilization of a system (Rawal, & Patel, 2018). The PDI is a measure of the heterogeneity of a lipid-nanocarrier reflecting size distribution affected by agglomeration or aggregation of lipid-nanocarriers. The numerical value of PDI ranges from 0.0 (for a perfectly uniform sample) to 1.0 (for a highly polydisperse sample). The narrow distribution PDI (values of 0.3 and below) is acceptable for lipid-based carriers (Danaei *et al.*, 2018). However, the PDI for all lipid-nanocarriers (0.441-0.572) indicated slightly broad size distributions, and their stability should be of concern. Furthermore, the physical stability of lipid-nanocarriers is usually predicted by the strength of surface charge that indicates the electrophoretic mobility of carriers. In general, the stable carriers tend to have either +30 or −30 mV. Particles with a large negative or positive zeta potential (more negative than −30 mV or more positive than +30 mV) will repel each other and will not aggregate (Jagdale & Pawar, 2017). The prepared NLCs and NEGs exhibited zeta potentials between −68.5 and −38.9 mV (Table 3), indicating that lipid-nanocarriers were stable. The electrostatic repulsion among the particles prevented their coalescence, ensuring the

Table 3. Physicochemical characterization of nanocarriers. All data are presented as mean ± SD (n = 3).

Formulation	Particle size (nm)	PDI	Zeta potential (mV)	pH	Conductivity (µs/cm)	Spreadability (g cm/min)
NLCs						
Blank-loaded	346.7 ± 45.3	0.441 ± 0.021	–45.0 ± 0.4	5.25 ± 0.01	26.10 ± 0.40	106.67 ± 2.89
Res-loaded	291.5 ± 39.2	0.523 ± 0.047	–46.7 ± 2.3	5.50 ± 0.01	28.40 ± 1.70	110.67 ± 5.13
NEGs						
Blank-loaded	269.2 ± 62.7	0.543 ± 0.034	–68.5 ± 2.5	5.58 ± 0.02	138.77 ± 0.83	193.02 ± 3.68
Res-loaded	160.0 ± 31.4	0.572 ± 0.056	–38.9 ± 1.0	5.54 ± 0.03	132.47 ± 0.21	199.11 ± 3.41
Gels						
Res-loaded	-	-	-	5.51 ± 0.02	347.33 ± 2.52	172.42 ± 1.86

physical stability of lipid-nanocarriers. Moreover, the attachment of lipid-nanocarriers to cell membrane seems to be most affected by the zeta potential. Lipid-nanocarriers with high negative zeta potential may repel the negatively charged domains of cell membranes. Nevertheless, there are a few cationic sites on cell membranes for adsorption of negatively charged lipid-nanocarriers. The negatively charged lipid-nanocarriers can bind at the cationic sites in the form of clusters for Res topical delivery (Honary, & Zahir, 2013). In addition, lipid-nanocarriers can bind by non-specific process on the cell membranes.

3.2.3 pH, conductivity and spreadability

The pH measurement was used to assess the non-irritating nature of the topical preparation when the product would be applied to the skin. The pH values of all formulations ranged from 5.25 to 5.58 (Table 3) close to the physiological pH of the skin (pH 5.5), indicating no irritation. The conductivity indicates the characteristics of the continuous phase of lipid-nanocarriers. The conductivity of formulations had the rank order NLCs < NEGs < gels. Gel formulation contained only water-soluble hydrophilic ingredients which made its conductivity the highest. PPM, a gelling agent was added into the NEs and increased conductivity of NEGs, compared to NLCs formulation.

The spreadability determines the comfort and ease in spreading the formulation onto skin. A large diameter indicates better spreadability. Average spreadability values of the formulations have been given in Table 3. The spreadability of formulations had rank order NLCs < gels < NEGs. NEGs contained both gelling agent and lipid components, which gave their high spreadability. Gels were second in spreadability due to the viscous PPM. The high solid and liquid content of NLCs made them difficult to spread, resulting in the lowest spreadability values. In addition, Res-loaded lipid-nanocarriers had slightly increased spreadability, indicating easy spreading of these formulations on the skin. Res might interact and interfere with the lipid core, resulting in increased spreadability. This might be attributed to the co-surfactant effect of Res (Souza *et al.*, 2011). Res might help in stabilization and spreadability of a system (Rawal, & Patel, 2018).

3.2.4 In vitro occlusive property and stability

Based on the results, NEGs were appropriate nanocarriers with the minimum particle size, stable carriers, and having a combination of good properties of gel and lipid-nanocarriers, thus these carriers were selected to evaluate *in vitro* occlusive property and stability. The occlusive factor of blank and Res-loaded NEGs was 51.16 ± 2.35 and 56.00 ± 2.44 %, respectively. The lipid contents of NEGs prevented water evaporation, led to increased skin hydration and promoted to the retention of moisture in the stratum corneum (Loo *et al.*, 2013). Moreover, the degree of occlusion on skin depended on the particle size of carriers, and the small particle size of Res-loaded NEGs provided less water evaporation from the skin leading to the higher occlusive effect than blank-loaded NEGs.

The stability of NEGs after storage for 3 months is presented in Figure 4. The appearance of NEGs presented the favored physical characteristics similar to the fresh preparation. The results indicate that the gel base had added thermodynamic stability to the NEs by increasing the viscosity of the aqueous phase and decreasing the interfacial and surface tension (Aithal, Narayan, & Nayak, 2016). The particle size of blank and Res-loaded NEGs slightly changed during storage for 3 months. In zeta-potential a decreasing trend was observed for blank and Res-loaded NEGs. However, the changes in particle size and zeta-potential were insignificant ($p > 0.05$).

Altogether, the NEGs provided good physicochemical properties for Res topical delivery, motivating future research towards the evaluation of entrapment efficiency, Res release, and skin permeation by Franz diffusion cell.

4. Conclusions

Res-loaded NLCs and NEs were successfully prepared by homogenization and ultrasonication techniques. The formulation components and process parameters exert significant influence on the HD of carriers. Stable carriers were prepared by homogenization at 6000 rpm for 5 min and ultrasonication processes. The emulsifier system of Tween®80, Span®80 and DGME provided good physical stability. The NEs could be prepared for Res-loaded NEGs with a minimum particle size and optimal zeta potential. PPM was the best gelling agent. Res was well loaded in the lipid matrix and provided satisfactory physical and chemical properties. NEGs were easy to spread on the skin and held water for at least 6 hours. The stability study revealed that the particle size and zeta potential of NEGs only insignificantly changed during storage for 3 months. Thus, these NEGs have the potential to be a nanocarrier for topical delivery of Res.

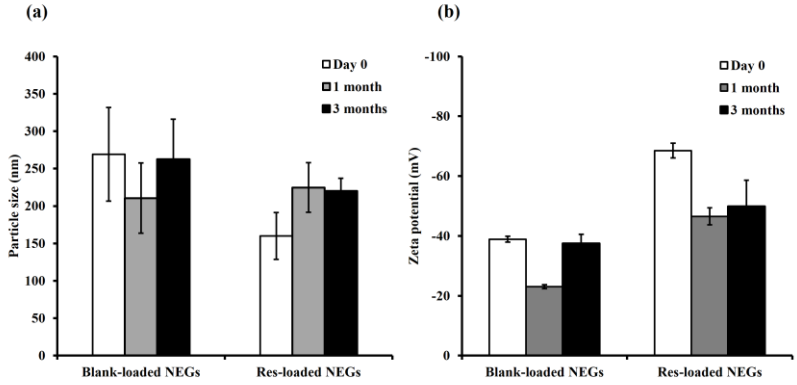

Figure 4. (a) Particle size, and (b) zeta-potential of blank and Res-loaded NEGs after preparation and storage at 4 ± 2°C for 3 months

Acknowledgements

This work was supported by the Thailand Science Research and Innovation (TSRI) through Research Team Promotion Grant (RTA6180003). The authors would like to acknowledge College of Pharmacy, Rangsit University for materials support. We also thank Kanyanut Chouthong, Ploypailin Charenpon, Napasorn Nakjaitham, Natrada Chutikunthanan and Watcharapong Thinchalong for their research assistance.

References

Aithal, G. C., Narayan, R., & Nayak, U. Y. (2016). Nanoemulgel: A promising phase in drug delivery. *Current Pharmaceutical Design*, *26*(2), 279-291. doi:10.2174/1381612826666191226100241

Aravand, M. A., & Semsarzadeh, M. A. (2008). Particle formation by emulsion inversion method: Effect of the stirring speed on inversion and formation of spherical particles. *Macromolecular Symposia*, *274*, 141-147. doi:10.1002/masy.200851419

Arora, R., Aggarwal, G., Harikumar, S. L., & Kaur, K. (2014). Nanoemulsion based hydrogel for enhanced transdermal delivery of Ketoprofen. *Advance Pharmaceutical Journal*, 468456. doi:10.1155/2014/468456

Bamba, B. S. B., Shi, J., Tranchant, C. C., Xue, S. J., Forney, C. F., Lim, L. T., Xu, W., & Xu, G. (2018). Coencapsulation of polyphenols and anthocyanins from blueberry pomace by double emulsion stabilized by whey proteins: Effect of homogenization parameters. *Molecules*, *23*(10), 2525. doi: 10.3390/molecules23102525

Benjasirimongkol, P., & Sriamornsak, P. (2016). Stability study of resveratrol-loaded emulsions using pectin as an emulsifier. *Asian Journal of Pharmaceutical Sciences*, *11*, 199-200. doi: 10.1016/j.ajps.2015.11.037

Chamsai, B., Samprasit, W., Opanasopit, P., Benja sirimongkol, P., & Sriamornsak, P. (2020). Types of solid lipids on physical stability of resveratrol-loaded nanostructured lipid carriers. *Key Engineering Materials*, *859*, 203-207. doi:10.4028/www.scientific.net/KEM.859.203

Danaei, M., Dehghankhold, M., Ataei, S., Davarani, F. H., Javanmard, R., Dokhani, A., Khorasani, S., & Mozafari, M. R. (2018). Impact of particle size and polydispersity index on the clinical applications of lipidic nanocarrier systems. *Pharmaceutics*, *10*, 57. doi:10.3390/pharmaceutics10020057

Han, L., & Wang, T. (2016). Preparation of glycerol monostearate from glycerol carbonate and stearic acid. *RSC Advances*, *6*, 34137–34145. doi:10.1039/C6RA02912D

Honary, S., & Zahir, F. (2013). Effect of zeta potential on the properties of nano-drug delivery systems - A Rreview (Part 1). *Tropical Journal of Pharmaceutical Research*,*12*(2), 255-264. doi: 10.4314/tjpr.v12i2.19

Imran, M., Iqubal, M. K., Imtiyaz, K., Saleem, S., Mittal, S., Rizvi, M. M. A., Alia, J., Baboot, S. (2020). Topical nanostructured lipid carrier gel of quercetin and resveratrol: Formulation, optimization, in vitro and ex vivo study for the treatment of skin cancer. *International Journal of Pharmaceutics*, *587*, 119705. doi: 10.1016/j.ijpharm.2020.119705

Jagdale, S., & Pawar, S. (2017). Gellified emulsion of ofloxacin for transdermal drug delivery system. *Advanced Pharmaceutical Bulletin*, *7*(2), 229-239. doi: 10.15171/apb.2017.028

Jiang, X., Hu, H., Bai, Y., Tian, X, Huang, D., & Wang, S. (2013). Synthesis and properties of the vinyl silicone oil modified polyacrylate core-shell latex as a binder for pigment printing. *Journal of Adhesion Science and Technology*, *27*(2), 154-164. doi:10.1080/01694243.2012.701527

Juškaité, V., Ramanauskiené, K., & Briedis. V. (2017). Testing of resveratrol microemulsion photostability and protective effect against UV induced oxidative stress. *Acta Pharmaceutica*, *67*(2), 247-256. doi: 10.1515/acph-2017-0018.

Kaur, A., Katiyar, S. S., Kushwah, V., & Jain, S. (2017).Nanoemulsion loaded gel for topical co-delivery of clobitasol propionate and calcipotriol in psoriasis. *Nanomedicine: Nanotechnology, Biology and Medicine*, *13*(4), 1473-1482, doi:10.1016/j.nano.2017.02.009.

Khoee, S., & Yaghoobian, M. (2009). An investigation into the role of surfactants in controlling particle size of polymeric nanocapsules containing penicillin-G in double emulsion. *European Journal of Medicinal Chemistry*, *44*(6), 2392-2399. doi:10.1016/j.ejmech.2008.09.045

Kubo, M. T. K., Augusto, P. E. D., & Cristianini, M. (2013). Effect of high pressure homogenization (HPH) on the physical stability of tomato juice. *Food Research International*, *51*, 170-179. doi:10.1016/j.foodres.2012.12.004

Loo, C. H., Basri, M., Ismail, R., Lau, H. L. N., Tejo, B. A., Kanthimathi, M. S., Hassan, H. A. & Choo, Y. M. (2013). Effect of compositions in nanostructured lipid carriers (NLC) on skin hydration and occlusion. *International Journal of Nanomedicine*, *8*, 13-22. doi:10.2147/IJN.S35648

López-García, R., & Ganem-Rondero, A. (2015). Solid Lipid Nanoparticles (SLN) and Nanostructured Lipid Carriers (NLC): Occlusive effect and penetration enhancement ability. *Journal of Cosmetics, Dermatological Sciences and Applications*, *5*, 62-72. doi:10.4236/jcdsa.2015.52008

Loureiro, J. A., Andrade, S., Duarte, A., Neves, A. R., Queiroz, J. F., Nunes, C., Sevin, E., Fenart, L., Gosselet, F., Coelhom, M. A. N., & Pereira, M. C. (2017). Resveratrol and grape extract-loaded solid lipid nanoparticles for the treatment of alzheimer's disease. *Molecules*, *22*(2), 277. doi:10.3390/molecules22020277

Neves, A. R., Lúcio, M., Martins, S., Lima, J. L.C., & Reis, S. (2013). Novel resveratrol nanodelivery systems based on lipid nanoparticles to enhance its oral bioavailability. *International Journal of Nanomedicine*, *8*, 177.187. doi: 10.2147/IJN.S37840

Rawal, S. U., Patel, M. M., (2018). Chapter 2 - Lipid nanoparticulate systems: Modern versatile drug carriers. In Grumezescu, A. M. (Ed), *Lipid Nanocarriers for Drug Targeting* (pp. 49-138). Amsterdam, Netherlands: William Andrew Publishing.

Rigon, R. B., Fachinetti, N., Severino, P., Santana , M. H. A., & Chorilli M. (2016). Skin delivery and in vitro biological evaluation of trans-resveratrol-loaded solid lipid nanoparticles for skin disorder therapies. *Molecules*, *21*, 116. doi: 10.3390/molecules21010116

Souza, L. G., Silva, E. J., Martins, A. L .L., Mota, M. F., Braga, R. C., Lima, E. M., Valadares, M. C., Taveira, S. F., & Marreto, R. N. (2011). Development of topotecan loaded lipid nanoparticles for chemical stabilization and prolonged release. *European Journal of Pharmaceutics and Biopharmaceutics*, *79*(1), 189-196. doi:10.1016/j.ejpb.2011.02.012

Subramaniam, B., Siddik, Z. H., & Nagoor, N. H. (2020). Optimization of nanostructured lipid carriers: understanding the types, designs, and parameters in the process of formulations. *Journal of Nanoparticle Research*, *22*, 141. doi: 10.1007/s11051-020-04848-0

Trivedi, M. K., Tallapragada, R. M., Branton, A., Trivedi, D., Nayak, G., Mishra R. K., & Jana, S. (2015). Physical, spectroscopic and thermal characterization of biofield treated myristic acid. *Journal of Fundamentals of Renewable Energy and Applications*, *5*, 180. doi:10.4172/20904541.1000180.9

Venuti, V., Cannavà, C., Cristiano, M. C., Fresta, M., Majolino, D., Paolino, D., Stancanelli, R., Tommasini, S., & Ventura, C. A. (2014). A characterization study of resveratrol/sulfobutyl ether-β-cyclodextrin inclusion complex and in vitro anticancer activity. *Colloids and Surfaces B: Biointerfaces*, *115*, 22-28. doi: 10.1016/j.colsurfb.2013.11.025

Vinothini, K., & Rajan, M. (2019). Chapter 9 - Mechanism for the nano-based drug delivery system. Characterization and biology of nanomaterials for drug delivery. In Mohapatra, S.S., Ranjan, S., Dasgupta, N., Mishra, R. K., & Amsterdam T. S. (Eds.), *Characterization and Biology of Nanomaterials for Drug Delivery* (pp. 219-263). Amsterdam, Netherlands: Elsevier.

Wei, Q., Yang, Q., Wang, Q., Sun, C., Zhu, Y., Niu, Y., Yu, J., & Xu, X. (2018). Formulation, characterization, and pharmacokinetic studies of 6-gingerol-loaded nanostructured lipid carriers. *AAPS PharmSciTech*, *19*(8), 3661-3669. doi:10.1208/s12249-018-1165-2